THE SEISMOLOGICAL SOCIETY OF AMERICA
400 Evelyn Ave., Suite 201
Albany, CA 94706-1375
(510) 525-5474; FAX (510) 525-7204
www.seismosoc.org

Bulletin of the Seismological Society of America, Vol. 99, No. 1, pp. 235–254, February 2009, doi: 10.1785/0120080059

Source Spectra and Site Response from *S* Waves of Intermediate-Depth Vrancea, Romania, Earthquakes

by Adrien Oth, Stefano Parolai, Dino Bindi, and Friedemann Wenzel

Abstract Seismograms from 55 intermediate-depth Vrancea earthquakes (M 4.0–7.1) recorded at 43 stations of an accelerometric network in Romania are used to derive source spectra and site amplification functions from *S* waves in the frequency range 0.5–20 Hz with the generalized inversion technique (GIT) (Castro *et al.*, 1990). Attenuation is taken into account using the nonparametric attenuation functions derived by Oth *et al.* (2008) from the same dataset, and the attenuation-corrected data are then split into source and site contributions. The source spectra follow the ω^{-2} model (Brune, 1970, 1971) with high corner frequencies and a related Brune stress drop of the order of 100 MPa. The site amplification functions are separately determined for both horizontal and vertical components. Contrary to widespread expectation, the vertical component shows significant amplification effects at high frequencies. The H/Z ratios determined from the GIT results compare well with H/V ratios computed directly from the *S*-wave window of the accelerograms (Lermo and Chávez-García, 1993). The basic assumption for the determination of site effects from H/V ratios is that the vertical component is not or only little affected by site effects. For Vrancea earthquakes, this assumption is incorrect; consequently, site effects should not be estimated from H/V ratios. The reason for this peculiar fact is the geometry of intermediate-depth seismicity that leads to almost vertical ray paths beneath the stations.

Introduction

The Vrancea seismogenic zone is located at the bend of the Carpathian mountain arc in Romania (Fig. 1). Here, frequent and strong intermediate-depth earthquakes occur within a narrowly confined focal volume (epicentral area of approximately 30×70 km^2, depth range of 80–200 km). Four such events with magnitudes larger than 6.5 took place during the last century, and the two earthquakes on 10 November 1940 (M_w 7.7) and 4 March 1977 (M_w 7.4) led to disastrous consequences, with more than 1500 fatalities on Romanian territory during the latter one (Cioflan *et al.*, 2004).

The severity of shaking due to an earthquake and, as a consequence, the estimated seismic hazard, depend on several factors, the most important of these being the radiation strength of the seismic source, the attenuation of the waves on their way from the source to the site of interest, and the near-surface amplification. A common method to isolate these three contributions from each other in the Fourier amplitude spectra (FAS) of ground motion is the generalized inversion technique (GIT), first proposed by Andrews (1986). Castro *et al.* (1990) introduced a two-step inversion method, where, in the first step, the path effects (i.e., attenuation) are isolated in terms of frequency-dependent, nonparametric attenuation functions, and source and site effects are separated in the second one after correcting the spectra for the obtained attenuation characteristics.

The GIT has been widely applied to crustal earthquake datasets (Castro *et al.*, 1990; Parolai *et al.*, 2000, 2004; Bindi *et al.*, 2006). Yet in the Vrancea case, the geometry of the dataset is very different from the crustal situation because the Vrancea earthquakes cluster in a small focal volume at intermediate depth and therefore, the ray paths from all hypocenters to a given station are practically identical. Furthermore, the smallest hypocentral distance (henceforth also called the reference distance) in the dataset amounts to roughly 90 km. As Oth *et al.* (2008) show, lateral inhomogeneities in the attenuation characteristics cannot be expected to average out due to this source-station geometry. To deal with this problem and to retrieve the attenuation characteristics beneath Vrancea, they introduced a modification in the first-step inversion scheme as compared with the original one of Castro *et al.* (1990). With this scheme, it is possible to account for variations in attenuation properties among the recordings from different sets of stations.

In order to separate source and site effects in the second step, the site amplification at one or more reference stations

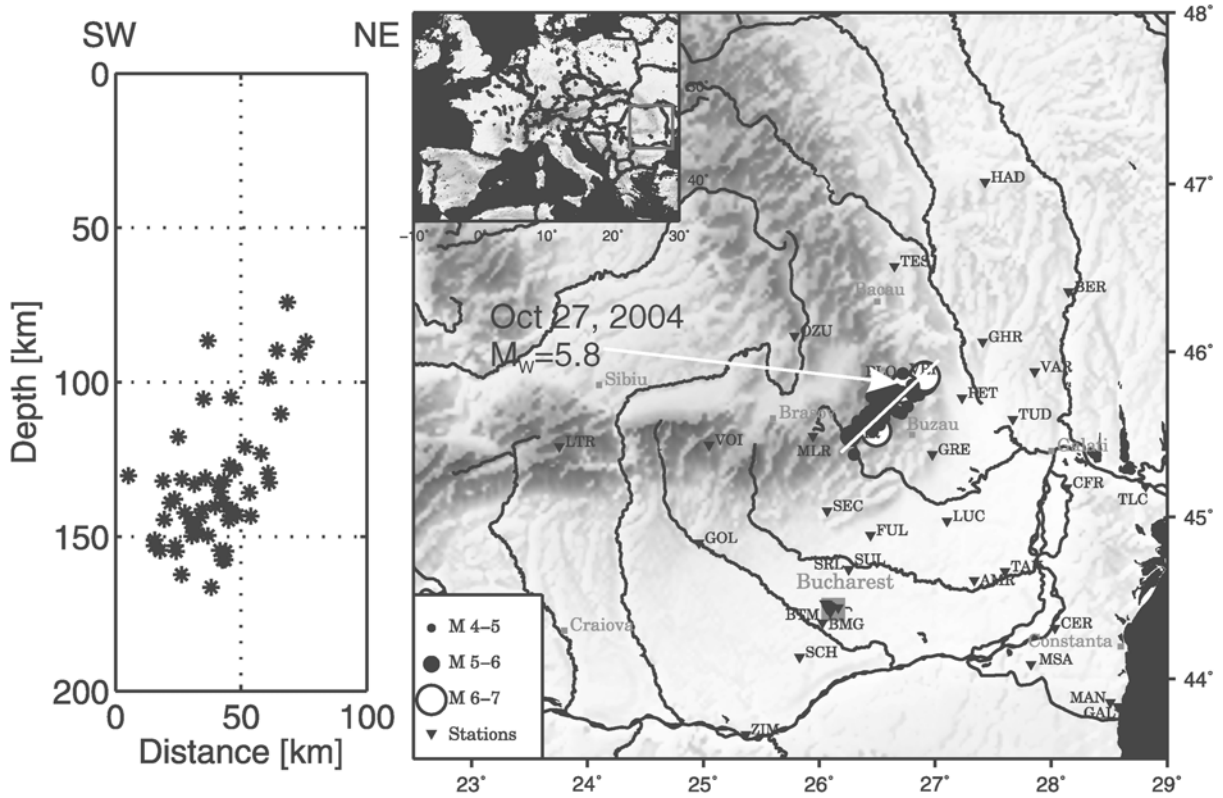

Figure 1. Map depicting the source-station configuration. The station locations are indicated as inverse triangles, whereas the epicenters are shown as circles. Left: southwest–northeast vertical cross section through the epicentral area. The cross section is marked by a white line on the map. The white arrow marks the epicenter of the 27 October 2004 (M_w 5.8) earthquake, which is used as a reference source when studying the source spectra.

is usually set to unity, as there is one undetermined degree of freedom that has to be fixed (Andrews, 1986). Thus, the obtained amplification functions are relative values with respect to this reference site. Another (nonreference) technique to estimate the site response is the H/V ratio method, which can be applied to both ambient seismic noise measurements (Nakamura, 1989) or *S*-wave spectra from earthquake recordings (Lermo and Chávez-García, 1993).

Studies dedicated to the comparison of different site response estimation techniques (e.g., Field and Jacob [1995]; Bonilla *et al.* [1997]; Parolai *et al.* [2004]) generally indicate that the H/V method is capable of revealing the fundamental resonance frequency of a site, but it often shows different amplitude levels than the results obtained using the GIT technique. However, if the vertical component is not free from amplification effects, the H/V method fails. These comparative studies have been performed with different datasets of crustal earthquakes, but no such comparison has been performed with such a peculiar dataset as the Vrancea one so far.

In this article, we describe the results obtained in the second step of the GIT from the Vrancea dataset, that is, the separation of source spectra and site response functions from the attenuation-corrected FAS. The obtained source spectra are corrected for the effect of the reference distance of 90 km and interpreted using the ω^{-2} model (Brune, 1970, 1971). We derive the site response functions from both the horizontal and vertical component spectra and compare them with the H/V ratios calculated from the same *S*-wave windows as used in the GIT inversion.

Dataset

The database used in this work is the same as employed by Oth *et al.* (2008) to study the seismic attenuation characteristics beneath Vrancea. More than 850 three-component accelerometric recordings from 55 Vrancea earthquakes at 43 stations spread over Romanian territory are used. Of these 55 events, 52 were recorded by the K2 network deployed in the framework of the Collaborative Research Center (CRC) 461: "Strong Earthquakes: A Challenge for Geosciences and Civil Engineering" since 1997. The records were corrected for instrumental response and band-pass filtered between 0.1 and 50 Hz, and their sampling rate is 200 samples/sec. In addition to the seismograms from these 52 events, strong-motion recordings from three large Vrancea earthquakes that occurred on 30 August 1986 (M_w 7.1, eight records), 30 May 1990 (M_w 6.9, eight records), and 31 May 1990 (M_w 6.4, three records) were included in the dataset. These strong-motion records were obtained by an analog SMA-1 network operated by the National Institute for Earth Physics

(NIEP) in Bucharest (Oncescu, Bonjer, *et al.*, 1999) and digitized at NIEP, having a sampling rate of 100 samples/sec.

The magnitude range of the events recorded by the K2 network with acceptable signal-to-noise ratio (SNR) ranges from 4.0 to 5.8. NIEP maintains and continuously updates the ROMPLUS catalog (Oncescu, Marza, *et al.*, 1999), which lists the hypocentral coordinates and moment magnitudes of the Vrancea events. Figure 1 shows the distribution of the epicenters of the considered earthquakes as well as a vertical cross section through the epicentral area. *S*-wave windows starting 1 sec before the *S*-wave onset (picked on the horizontal components) and ending when 80% of the record's total energy is reached were selected and a 5% cosine taper applied. Typical window lengths range from 5 to 15 sec. If the determined window was longer than 20 sec, its duration was fixed to be 20 sec to avoid having too much coda energy in the analyzed windows. For each window, the FAS was calculated and smoothed around 30 frequency points equidistant on a logarithmic scale between 0.5 and 20 Hz using the windowing function of Konno and Ohmachi (1998) with $b = 20$. Preevent noise windows of equal length as the signal windows were used to compute the SNRs, and at each frequency point, only records with an SNR higher than 3 were retained. Below 0.5 Hz, too few records had an acceptable SNR (for the smaller events, the SNR was mostly smaller than 1.5–2 below 0.5 Hz). For the horizontal (H) components, the root-mean-square (rms) average of the north–south and east–west components is used in the final dataset. At each of the 30 frequency points, only events recorded by at least three stations and only stations that recorded at least three events with acceptable SNR were kept in the dataset. As a result of this selection criterion based on the SNR, a few source and site spectra are incomplete either at the highest (> 12 Hz) or lowest (< 1 Hz) frequencies with respect to the frequency range analyzed (0.5–20 Hz).

Figure 2 shows two example recordings from the 27 October 2004 (M_w 5.8) earthquake (depth approximately 100 km) at stations PET and AMR. As already discussed in Oth *et al.* (2008), almost no *S*-wave energy is seen on the vertical (Z) component in many cases (see station PET in Fig. 2). The *P* wave, due to the near-vertical incidence, often shows large amplitudes, with a peak in the FAS around 8–10 Hz. Some stations in the forearc area occasionally depict strong high-frequency arrivals on the Z component around 5–8 sec before the *S*-wave arrival (see also Oth *et al.* [2008], Fig. 2). These could be interpreted as *S*-*P* conversions at the base of the Focsani basin (the basin sediments reach to a depth of up to 8 km and up to 22 km including Mesozoic cover; Hauser *et al.*, 2007). However, the seismic *P*-wave velocity contrast estimated by Hauser *et al.* (2007) at the bottom of the basin is not strong enough to justify the amplitude of the observed phase. Furthermore, the observed time difference of 5–8 sec would imply a v_P/v_S ratio between 2 and 3 within the basin, according to the v_P model of Hauser *et al.* (2007). Although a deeper analysis of these identified phases might shed light on the knowledge of the geological structure, due to the lack of more detailed information and to the aim of the present article, we refrain from a further discussion of these phases. The missing *S*-wave energy on the Z component, besides the geometry of the dataset, especially distinguishes the Vrancea seismograms from typical recordings of crustal earthquakes. Figure 3 in Oth *et al.* (2008) shows several examples of the chosen *S*-wave windows and the respective FAS.

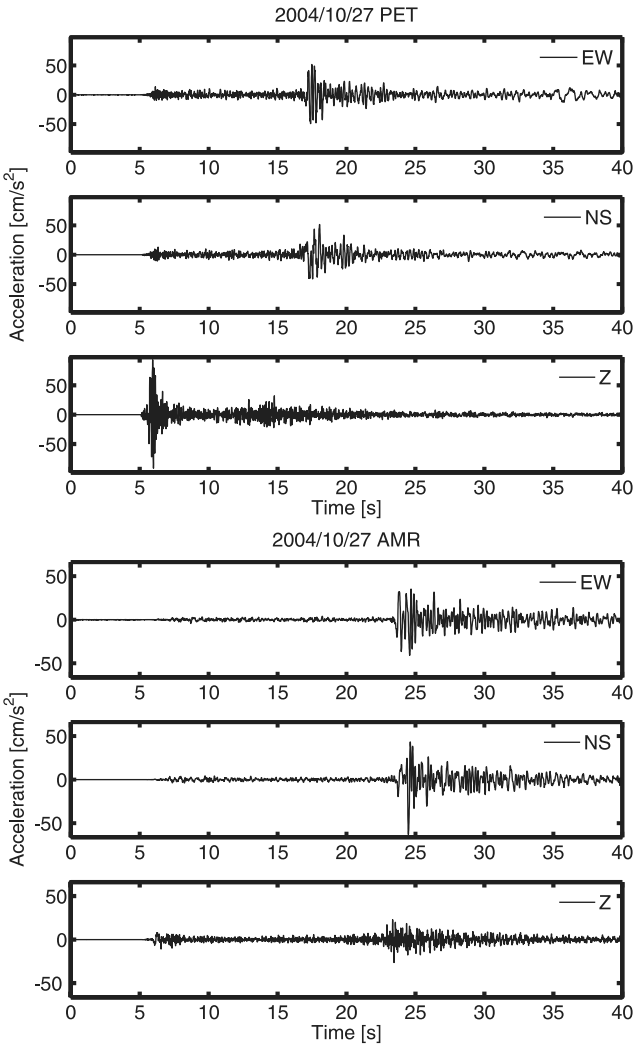

Figure 2. Three-component accelerograms of the 27 October 2004 (M_w 5.8, depth 100 km) earthquake at stations PET and AMR. Note that the origin of the time axis does not correspond to the origin time of the earthquake, but it has been adjusted for viewing purposes.

Methods

Generalized Inversion Technique

We apply the nonparametric GIT (Castro *et al.*, 1990) to derive attenuation characteristics, source spectra, and site response functions. The inversion is split into two steps: in the first, the dependence on the distance of the spectral amplitudes at a given frequency is modeled by

$$U_{ij}(f, r_{ij}) = A(f, r_{ij})\hat{S}_j(f), \quad (1)$$

where $U_{ij}(f, r_{ij})$ is the spectral amplitude (acceleration) at the ith station resulting from the jth earthquake, r_{ij} is the source-site distance, $A(f, r_{ij})$ is the function describing attenuation along the path from source to site, and $\hat{S}_j(f)$ is a scalar that depends on the size of the jth event. Equation (1) can be linearized by taking the logarithm, leading to a linear system of the form $\mathbf{Ax} = \mathbf{b}$, which can be solved, for example, with singular value decomposition (Menke, 1989). The first-step inversion applied to the Vrancea dataset is discussed in detail in Oth *et al.* (2008). There, it is shown that in the Vrancea case, lateral heterogeneities in the attenuation characteristics must be taken into account in the inversion scheme. Oth *et al.* (2008) derive different attenuation functions for two distinct regions, where region 1 is mainly given by the forearc area of the Carpathian mountain arc and region 2 is roughly restricted to the epicentral area. In this article, we focus on the second step of the inversion, destined to separate source spectra and site amplification functions.

Once $A(f, r_{ij})$ has been determined, the spectral amplitudes at each frequency can be corrected for the effect of seismic attenuation (with the attenuation functions derived in Oth *et al.* [2008]) and, in the second inversion step, the corrected spectra are split into source spectra and site transfer functions (Andrews, 1986):

$$R_{ij}(f) = S_j(f)Z_i(f). \quad (2)$$

Here, $R_{ij}(f) = U_{ij}(f, r_{ij})/A(f, r_{ij})$ are the spectral amplitudes after the correction for path effects, $S_j(f)$ is the source spectrum of the jth earthquake, and $Z_i(f)$ is the site amplification function at station i. In the Vrancea case, the spectral amplitudes are corrected with the appropriate attenuation functions for the respective region in which the station under consideration is located (Oth *et al.*, 2008). Furthermore, it is important to note at this point that the correction for path effects can only be done for distances larger than the reference distance. For crustal datasets, this reference distance is often set to zero if several data points are available at small hypocentral distances. However, this is not the case in this study, with a smallest hypocentral distance of 90 km. Thus, the attenuation-corrected spectra still include a cumulative attenuation effect over a distance of 90 km, which will be important for the discussion of the source spectra in the following section.

Again, equation (2) can be transformed into a linear system by taking the logarithm

$$\log_{10} R_{ij}(f) = \log_{10} S_j(f) + \log_{10} Z_i(f). \quad (3)$$

As Andrews (1986) notes, there is one undetermined degree of freedom that needs to be fixed. Either (at least) one source spectrum or one site amplification function has to be specified to remove this indetermination. A common constraint is to set the site response of a rock site to one (respectively zero in $\log_{10}$), irrespective of frequency, or to set the average site amplification of a set of stations to one (Castro *et al.*, 1990). We use the constraint that the average site amplification of stations SIR (covered by the circles marking the epicenters in Fig. 1) and MLR be one, as these two stations are classified as rock stations and the H/V ratios presented later in this article are roughly flat and close to unity.

For each inversion (i.e., at each frequency point), the stability of the results is evaluated by bootstrap analysis (Efron and Tibshirani, 1994). Bootstrap methods work by repeated inversions of resampled versions of the original dataset. From the original dataset, a new one is created by randomly choosing rows from the linear system, where each row can either be selected several times or never. Further details on the procedure can be found in Parolai *et al.* (2000, 2004). The rows containing the previously mentioned constraints remain unchanged. At each frequency, we perform 200 bootstrap inversions and compute the mean and standard error for each model parameter.

H/V Ratios from Earthquake Recordings

The H/V ratio technique, basically consisting in computing the ratio of the FAS of the horizontal and vertical components of ground motion, has been widely applied in recent years in order to assess local site amplification effects. This method assumes that the vertical component of ground motion is not severely affected by local site conditions and hence, the H/V ratio can be used as an estimate of site amplification of the horizontal ones. It was made popular by Nakamura (1989) for ambient noise measurements; Lermo and Chávez-García (1993) first applied the technique to the S-wave part of earthquake recordings and studied the theoretical basis of the approach by numerical modeling of SV waves. Since then, the H/V technique has been applied to earthquake recordings worldwide (e.g., Theodulidis and Bard [1995]; Chen and Atkinson [2002]; Siddiqqi and Atkinson [2002]; Sokolov *et al.* [2005]).

Comparative studies between the H/V ratio and other methods of site response estimation (e.g., Field and Jacob [1995]; Bonilla *et al.* [1997]; Parolai *et al.* [2004]) show that, generally, the H/V technique is able to reveal the predominant frequency peaks in the site amplification function, even though the amplitude level may be different from the site response functions obtained with the GIT. Yet this is only true as long as the vertical component is not affected by amplification effects. Parolai and Richwalski (2004) provide a theoretical explanation of why H/V fails in correctly estimating the level of amplification at frequencies higher than the fundamental one (transfer of energy on the vertical component due to S-P conversions at the bottom of the soft layer). Furthermore, as Parolai *et al.* (2004) note, reliable estimates of site amplification can only be derived from the H/V ratio if the sources are well distributed all around the station at different distances, as the H/V ratio depends on the inci-

dence angle of the seismic waves (Lermo and Chávez-García, 1993). This is clearly not the case for the Vrancea dataset. In order to clarify the relation between the H/V ratios and the GIT site amplification functions in this special case, we compute the H/V ratios from the same S-wave windows as used in the GIT inversion (see the Dataset section) and compare them with the site transfer functions obtained from the GIT.

Source Spectra of Vrancea Earthquakes

As previously mentioned, in order to remove the undetermined degree of freedom in the second step inversion in equation (3), we use the constraint that the logarithmic sum of site effects of stations MLR and SIR be zero. Yet the attenuation-corrected ground-motion spectra still contain a cumulative attenuation effect over the reference distance of 90 km (the lowest hypocentral distance in the dataset; see also Oth *et al.*, [2008]). As this effect is not taken into account with the constraint on the site response functions, it is moved into the inverted source contributions. Therefore, in order to derive estimates of the source spectra, this attenuation over the reference distance has to be corrected.

If the true source spectrum of one of the events were known, it would be possible to derive a correction term at each analyzed frequency point. Oth *et al.* (2007) used the large amount of accelerograms recorded from the moderate shock (M_w 5.8) that occurred on 27 October 2004 to estimate the corner frequency of this earthquake from the spectral ratios between the latter earthquake and appropriate empirical Green's functions (EGF) recordings. They obtained a shape of the spectral ratios consistent with the ω^{-2} model (Brune, 1970, 1971) for the source spectrum and a stable corner frequency estimate around 1.6 Hz for the 2004 shock, while using two different EGFs. This value of the corner frequency is very large for an event of M_w 5.8, indicating large stress drops for Vrancea earthquakes (Oncescu, 1989; Oth *et al.*, 2007).

As the source spectrum of the 27 October 2004 earthquake (ω^{-2} shape, seismic moment M_0 corresponding to M_w 5.8 following Hanks and Kanamori [1979], and corner frequency $f_C = 1.6$ Hz) is the best constrained one in the case of Vrancea earthquakes, we use it as a reference source spectrum to derive a correction term $\Psi(f)$ from the inverted source contribution $S_{2004\ \mathrm{event}}(f)$ following the equation:

$$\Psi(f) = S_{2004\ \mathrm{event}}(f)/(2\pi f)^2 \frac{\Re^{\theta\phi} VF}{4\pi\rho v_S^3} M_0 \left[1 + \frac{f^2}{f_C^2}\right]^{-1}, \quad (4)$$

where $\Re^{\theta\phi}$ is the average radiation pattern set to 0.6, $V = 1/\sqrt{2}$ accounts for the separation of S-wave energy on two horizontal components, $F = 2$ is the free surface amplification, $\rho = 3.2$ g/cm^3 is the density, and $v_S = 4.5$ km/sec is the shear-wave velocity in the source region. $\Psi(f)$ contains geometrical spreading, anelastic, and possibly scattering attenuation over the reference distance. No high-frequency decay, which is usually accounted for by the exponential κ operator (e.g., Anderson and Hough [1984]; Boore and Joyner [1997]; Boore [2003]) in spectral ground-motion models, has been accounted for when setting the site constraint at MLR and SIR. Therefore, $\Psi(f)$ may also contain the effect of κ at the rock stations MLR and SIR. The issue of κ is further treated in the following section, when the results for the site amplification functions are discussed.

The inverted source contribution from the 27 October 2004 event as well as $\Psi(f)$ are displayed in Figure 3. The inverted source contributions of the remaining events are then corrected for $\Psi(f)$ and the constants in equation (4) to obtain the corrected source spectra $S_{j,\mathrm{corrected}}(f)$ related to the inverted source contributions $S_{j,\mathrm{inverted}}(f)$ by

$$S_{j,\mathrm{corrected}}(f) = \frac{4\pi\rho v_S^3}{(2\pi f)^2 \Re^{\theta\phi} VF} \times \frac{S_{j,\mathrm{inverted}}(f)}{\Psi(f)}. \quad (5)$$

Figure 4 shows the inverted source spectra at the reference distance on the left and the corrected source spectra following equation (5) on the right for three events from the dataset. Except at the highest frequency, the error estimates derived from the bootstrap analysis are small and hence, the source contributions obtained from the inversion are well constrained. To the corrected source spectra depicted as circles on the right in Figure 4, we fit ω^{-2} spectra (Brune, 1970, 1971) using nonlinear least squares to derive the seismic moment M_0 and the corner frequencies f_C of the earthquakes in the dataset. For the three largest events in the dataset with M_w 7.1, 6.9, and 6.4, the corner frequencies are most likely lower than the lowest analyzed frequency. As a result, the derived source functions only show the acceleration plateau of the spectrum that could be explained with any combination of M_0 and f_C. Therefore, the spectral fitting was performed constraining M_0 to the value obtained using the moment magnitudes from the ROMPLUS catalog (Oncescu, Marza, *et al.*, 1999) and the relation of Hanks and Kanamori (1979) between M_0 and M_w.

The corner frequencies obtained by fitting ω^{-2} models to the corrected spectra are plotted versus seismic moment M_0 in Figure 5 (top; the error bars are indicative of the regressional error of the fit). The corner frequencies are generally very high, indicating large values of stress drop. Computing the Brune (1970, 1971) stress drop leads to values ranging around 100–200 MPa. Note, however, that the absolute values of stress drop derived from the spectra of seismic waves are strongly model dependent, as discussed by Beresnev (2001, 2002). Yet as the corner frequencies obtained for Vrancea earthquakes are much higher than the values typically found for crustal earthquakes (see, e.g., Miyake *et al.* [2003] for some typical values), one can say with a high degree of confidence that Vrancea earthquakes indeed display larger stress drops than typical crustal events. For instance, following the Brune (1970, 1971) model, which leads to the relation $\Delta\sigma = 8.5 M_0 f_C^3 / v_S^3$, where $\Delta\sigma$ is the stress drop, a corner frequency f_C ranging between 1–2 Hz (depending on

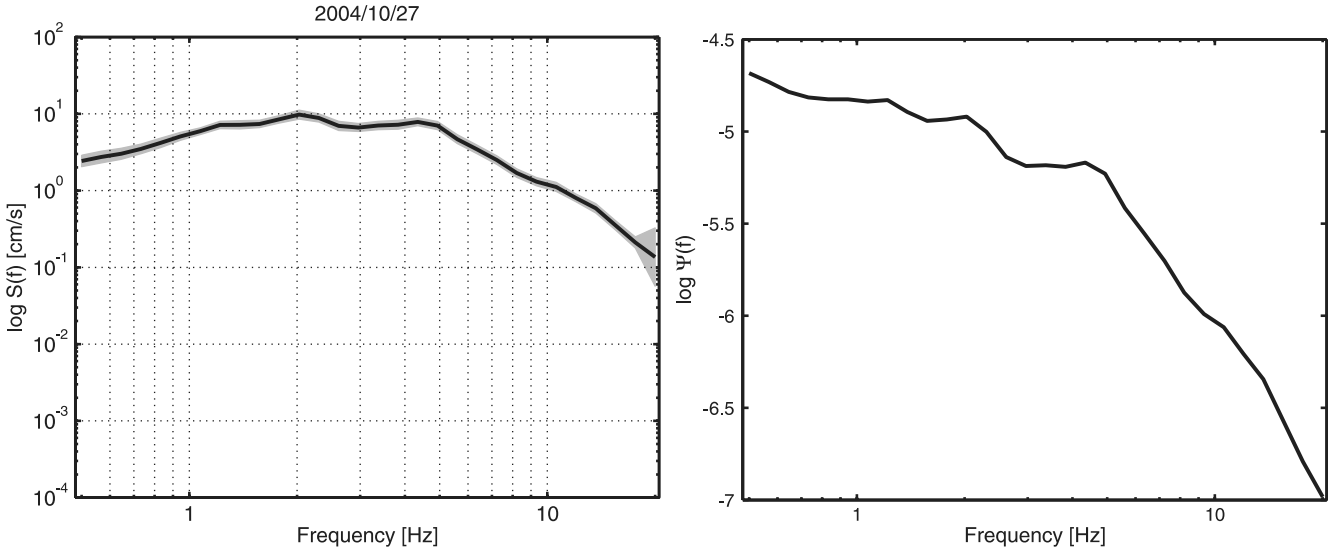

Figure 3. Left: inverted source contribution for the 27 October 2004 (M_w 5.8) earthquake. This source function still contains attenuation effects over the reference distance of 90 km. Right: logarithm of the correction function $\Psi(f)$ versus frequency. More information is provided in the text.

the shear-wave velocity estimate v_S) would be expected for an M_w 4.0 earthquake with a stress drop of 1 MPa, which is the order of magnitude generally assumed for crustal earthquakes (Kanamori, 1994). A Vrancea event of this magnitude, on the other hand, depicts values of f_C around 8–10 Hz.

The large stress drops for Vrancea earthquakes are in good agreement with the results presented by Oth *et al.* (2007) from a study of the source parameters of several Vrancea earthquakes using EGFs. They also derive stress-drop estimates ranging around 100 MPa. Furthermore, Oncescu (1989), applying different methods to estimate the stress drop of the large Vrancea earthquake that occurred on 30 August 1986, comes to similar conclusions. By fitting a straight line to $\log f_C$ plotted against $\log M_0$, the slope is approximately equal to the one expected in the case of self-similarity, that is, roughly $-1/3$. Note, however, that this trend is mainly determined by events with $M_w < 5.5$, as only a few stronger earthquakes are in the dataset. The spectral scaling analysis between large and small Vrancea earthquakes discussed in Oth *et al.* (2007) also indicates roughly self-similarity among Vrancea earthquakes. In fact, from the spectral ratios between the FAS of the recordings of large events and appropriate EGFs, they derive the stress-drop ratio C between large and small events varying between 0.7 and 2 ($C = 1$ would mean self-similar scaling).

The difference in stress drop between common crustal earthquakes and the Vrancea events analyzed here (occurring in the depth range between 80 and 200 km, so far below the crust, which has a thickness of about 35–45 km; Hauser *et al.*, 2007) may be related to the tectonic setting of the study area. The tectonic setting of the Vrancea region is considered to be the result of a retreating subduction zone with subsequent soft continental collision and slab rollback (Sperner *et al.*, 2001). The continent–continent collision formed the Carpathian mountain arc (Fig. 1). The break-off of the subducted lithosphere is believed to cause the strong seismicity at intermediate depth, which occurs in a slab segment not yet completely detached. This interpretation is compatible as well with the observed focal mechanisms (indicating a thrust regime with horizontal compression and vertical extension; e.g., Constantinescu and Enescu [1964]; Oncescu and Bonjer [1997]) and the regional seismic tomography results of Martin *et al.* (2006), which image the slab and show that the seismicity is confined to the slab. Stress drops of earthquakes occurring in the subducted lithosphere seem to be larger than those of crustal earthquakes. For instance, García *et al.* (2004) also observe systematically larger stress drops for in-slab earthquakes in Mexico as compared with crustal events.

The seismic moments M_0 were also derived from the source spectra. The bottom plot in Figure 5 shows the moment magnitude M_w derived from the spectra (inferred from M_0 using the relation of Hanks and Kanamori [1979]) plotted versus the moment magnitude from the ROMPLUS catalog (Oncescu, Bonjer, *et al.*, 1999). The moment magnitudes obtained from the spectra in this study follow the linear trend well where they would be identical to the ones from the catalog (with maximum differences in the order of 0.3–0.5 magnitude units). As previously mentioned, the seismic moments of the largest events were constrained when fitting the source spectra with the ω^{-2} model, which is why for these earthquakes, the values of M_w are of course identical to the ones from the catalog.

The previously discussed source properties have been derived only from the horizontal component spectra. The source functions obtained from the inversion of the vertical component are somewhat different, because there is only little S-wave energy on many records on the vertical component, as explained in the Dataset section. Thus, the source

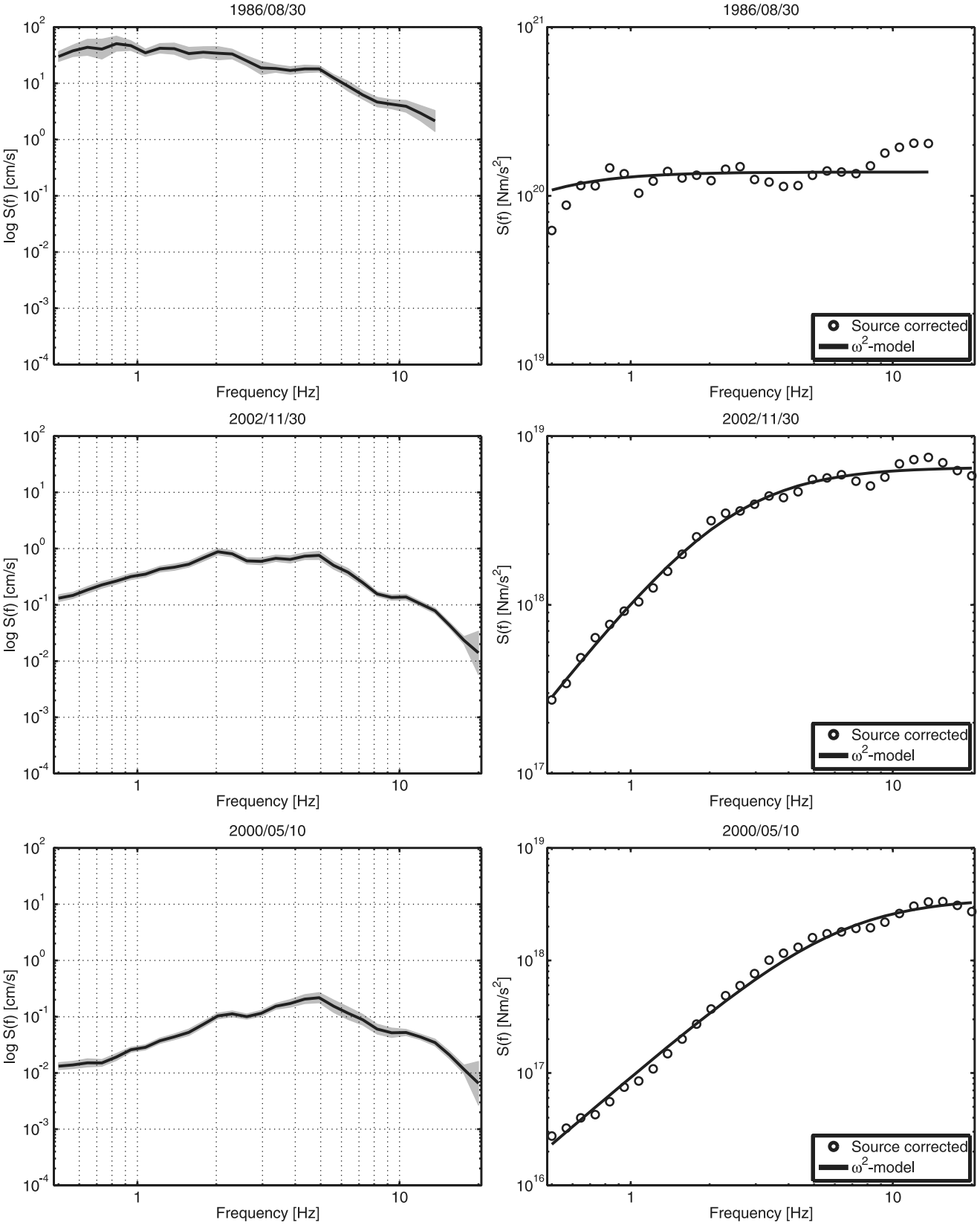

Figure 4. Inverted source contributions (left) and acceleration source spectra after correction of attenuation over the reference distance with $\Psi(f)$ (right) for three example earthquakes (30 August 1986: M_w 7.1, 30 November 2002: M_w 4.7, and 10 May 2000: M_w 4.1). The black line in the right-hand-side figures indicates the theoretical ω^{-2} model fitted to the source spectra.

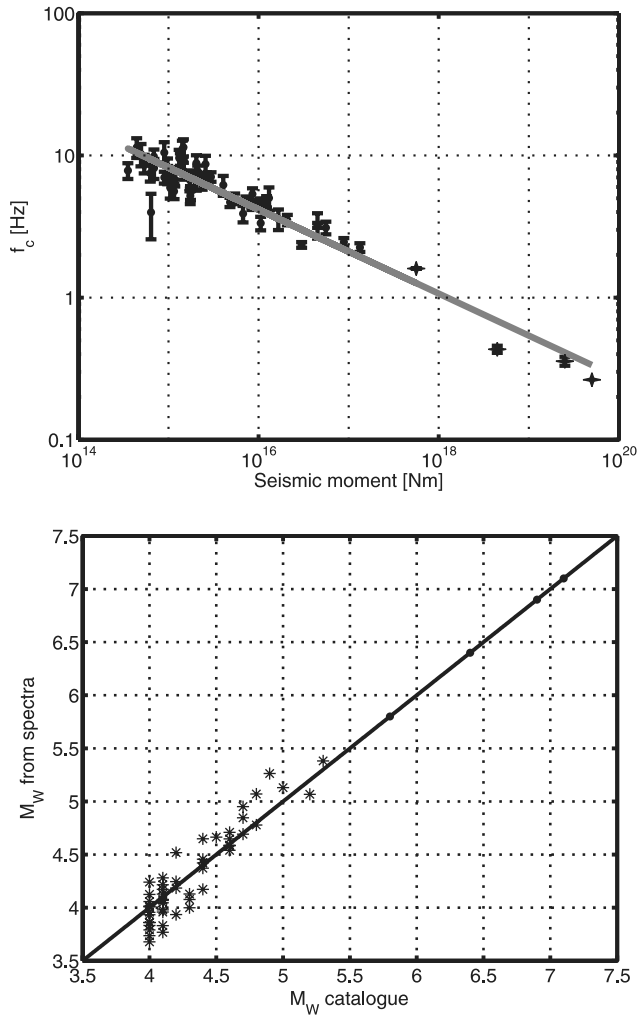

Figure 5. Top: corner frequency versus seismic moment. The fitted straight line has a slope of -0.3, close to the expected value of $-1/3$ in the case of self-similar scaling. Note, however, that there are only a few data points available at large magnitudes. Bottom: moment magnitude from the ROMPLUS catalog (Oncescu, Marza, *et al.*, 1999) versus moment magnitude derived from the source spectra. The trend follows the straight line where they are identical. Note that the moment magnitudes of the four largest events have been constrained to the values from the catalog when fitting the spectra (different symbols are used in both graphs for the four largest earthquakes).

functions obtained from the vertical component are, in fact, not representative of *S*-wave source spectra; therefore, the source properties are only discussed using the results obtained from the horizontal components. Yet there is a signal on the vertical component, and this signal is exploitable to estimate site transfer functions, even though the source functions obtained from the inversion of this signal are not the source functions of direct *S* waves.

Site Response—GIT Results

The site amplification functions have been derived using the GIT both from the horizontal (H) and vertical (Z) component spectra. In both cases, the constraint used in the inversion is that the logarithmic sum of the site response functions at stations SIR and MLR equals zero, that is, the average site response of these two stations equals unity. This site constraint can be regarded as reasonable because the H/V ratios are roughly flat and approximately equal to unity (Fig. 6). Strictly speaking, this does not necessarily mean that these sites are free from amplification effects, because similar results could be obtained if the horizontal and vertical components are amplified in an equal fashion. Yet the observation of flat H/V ratio in combination with the fact that these two stations are rock sites justifies the assumption of unit site response. Nevertheless, it should be pointed out that all site amplification functions (as well as the source spectra treated previously) are relative to the assumed average at these two sites.

The obtained site response functions for the H component are shown at several sites in the forearc region in Figure 7 and at the sites in the epicentral area in Figure 8 (which are regions 1 and 2, respectively, in Oth *et al.* [2008]). Figures 9 and 10 depict the results for the Z component at the same stations. The bootstrap analysis indicates that the results are very stable, except for the highest frequency on the H component where the standard deviation is somewhat larger. As expected, the amplification for MLR and SIR ranges around their average value one, as imposed by the constraint. A typical observation, both for the H and even much stronger for the Z component, is the high level of amplification at high frequencies. For the H component, the amplification increases generally with frequency (e.g., VRI, SEC, LUC, or CER) and stays on a high level, also at frequencies larger than 10 Hz. On the Z component, it is often observed that especially at these very high frequencies, the amplification strongly rises. The maximum amplification on the Z component is generally shifted to higher frequencies than on the H component. For several stations, the amplification of the H component from the GIT is more or less continuous over a large frequency band (e.g., SEC and BMG).

This strong amplification at high frequencies could be partially due to the fact that no κ operator (e.g., Anderson and Hough [1984]; Boore and Joyner [1997]) has been taken into account when setting the site constraint for the two rock sites. For instance, Hartzell *et al.* (1996) constrained a hard rock site to show an amplification equal to 1 and a κ-related high frequency diminution, with $\kappa = 0.02$. The differential κ due to a different near-surface attenuation at different sites should, however, be reflected by the presented site amplification functions. Introducing κ for rock stations into the site constraint would lead to a fall off of all site functions at high frequencies (with the same κ effect for all stations) and increase the high-frequency level in the source spectra; but relative to each other, nothing would change in the site functions.

κ is strongly dependent on the site conditions, reflecting attenuation in the near-surface weathered layers (Anderson and Hough, 1984), but also, source (Papageorgiou and Aki,

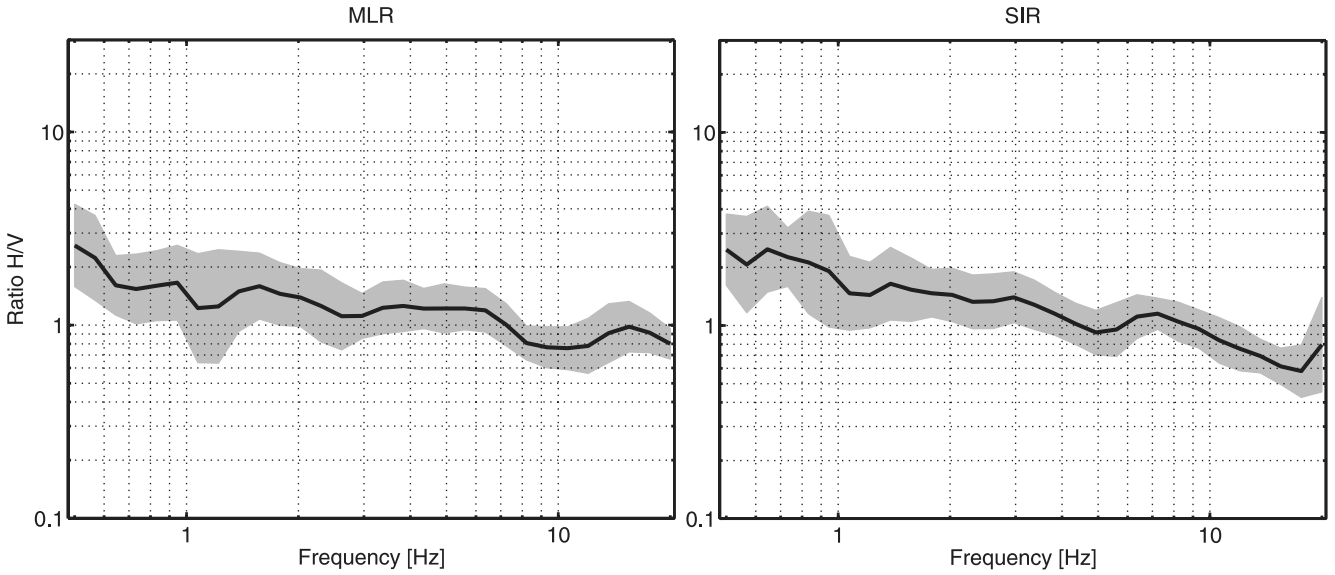

Figure 6. H/V ratios at rock stations MLR (left) and SIR (right). The black line marks the mean value derived from all considered events and the gray shaded area indicates the standard deviation.

1983) and propagation (Hanks, 1982) effects can lead to a high-frequency decay in the acceleration spectra, deviating from the ω^{-2} model. Purvance and Anderson (2003) show that κ can be parameterized as a combination of a distance-, a site-, and a source-dependent term. These terms can, in principle, be separated from each other with a similar inversion scheme as used in this work. However, the measured values of κ from the high-frequency decay of the spectra should be unaffected by site amplification effects (as Parolai and Bindi [2004] show, the fundamental resonance frequencies of the site must be well below the frequency band used for the determination of κ, and the frequency band used must be large enough in order to avoid that the measured κ values are solely determined by the slope of peaks in the site response curve) and must be measured well above the corner frequency of the respective event. Even at high frequencies (above 10 Hz), considerable site effects are observable in Figures 7, 8, 9, and 10. Moreover, as discussed in the preceding section and by Oth *et al.* (2007), the corner frequencies of the smaller events tend to be very high, too. Therefore, we refrain from further discussing κ measured from the high-frequency fall off of the spectra.

Several examples for the fit between observed spectra and the inverted spectral model (multiplying the terms for source, attenuation, and site derived above with each other) are shown in Figure 11. Generally, the agreement is fair to excellent, although in a few cases the spectral amplitude in parts of the spectrum is misestimated up to a factor of around 2–3. Very few outliers show a stronger misestimation (only 5% of the spectra show a misestimation in amplitude higher than a factor 3.5 at some given frequency—it is not the entire spectrum that is misestimated).

H/V Results and Comparison with GIT Site Response

In the case of the Vrancea earthquakes, the site amplification functions for the Z component derived using the GIT show severe amplification effects, especially at high frequencies. Moreover, the source-to-station geometry is very special: due to the strong clustering in space and the depth of the hypocenters, the incidence angles do not vary a lot (always near-vertical incidence) as compared with the case of crustal earthquakes; in addition, the sources are not at all distributed around a given station. Rather, waves travel very similar paths for a given site. Moreover, as discussed before, the Z component does not carry much S-wave energy. For these reasons, it may be questionable whether the H/V ratio technique, applied to Vrancea earthquakes, provides reliable estimates of site amplification.

Indeed, if one directly compares the H/V ratios (Fig. 12) with the amplification functions obtained for the H component (Figs. 7 and 8), strong differences can immediately be recognized, especially at higher frequencies. For instance, at station CER (H component), the site function from the GIT increases in the frequency range 1–2 Hz and remains at a level of approximately 7–8 for higher frequencies. The H/V ratio, on the other hand, indicates an isolated peak slightly shifted to lower frequencies (1.5–2 Hz) and almost no amplification at all at higher frequencies. In general, the H/V ratio underestimates the site amplification of the H component obtained from the GIT both in shape and in amplitude (especially at high frequencies).

If the site amplification on the Z component is not approximately one, then the H/V ratio should simply represent the amplification of the H component divided by the one of

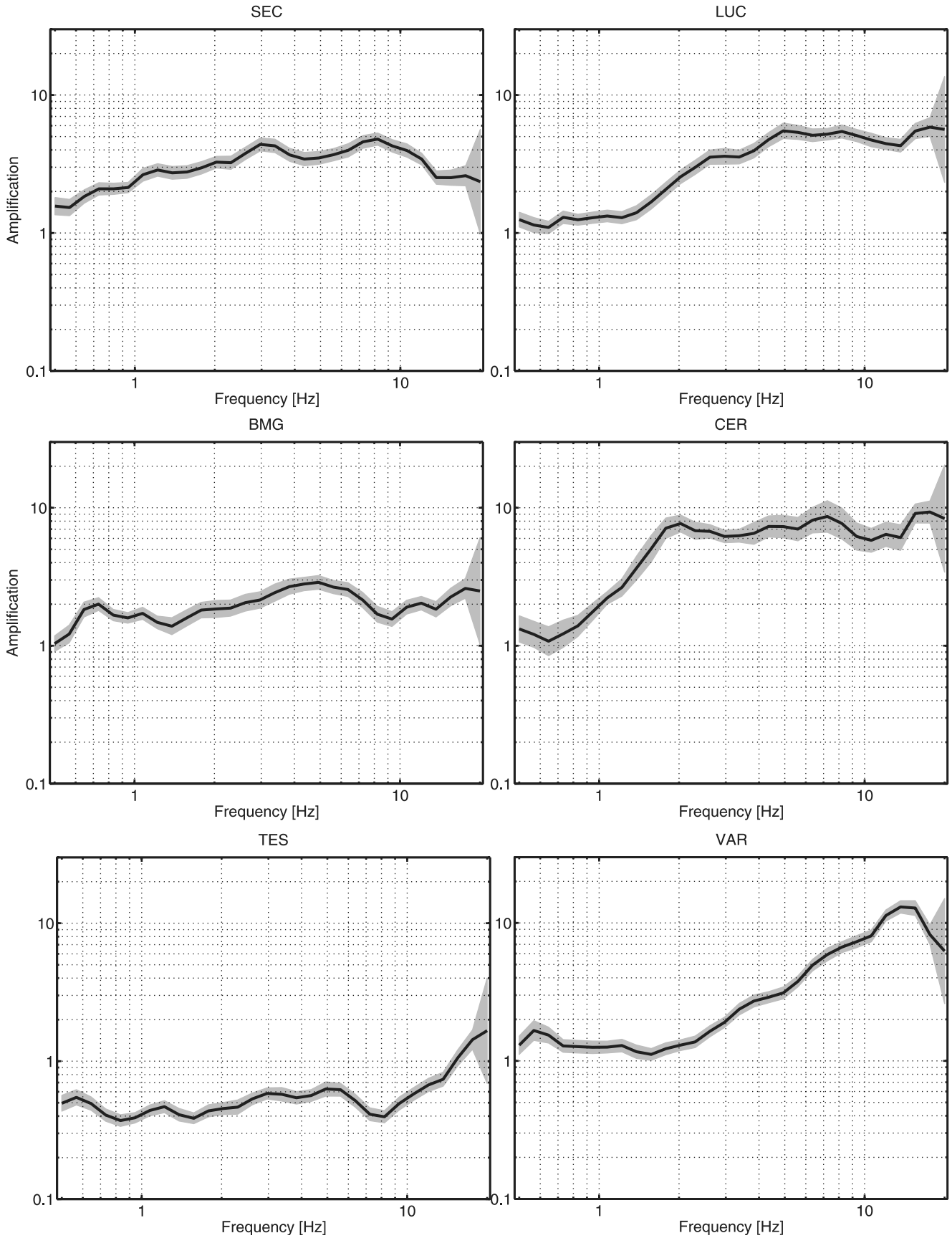

Figure 7. Site amplification functions obtained from the horizontal component at six stations in the forearc region. Black line: mean of 200 bootstrap samples. Gray shaded area: mean ± one standard deviation.

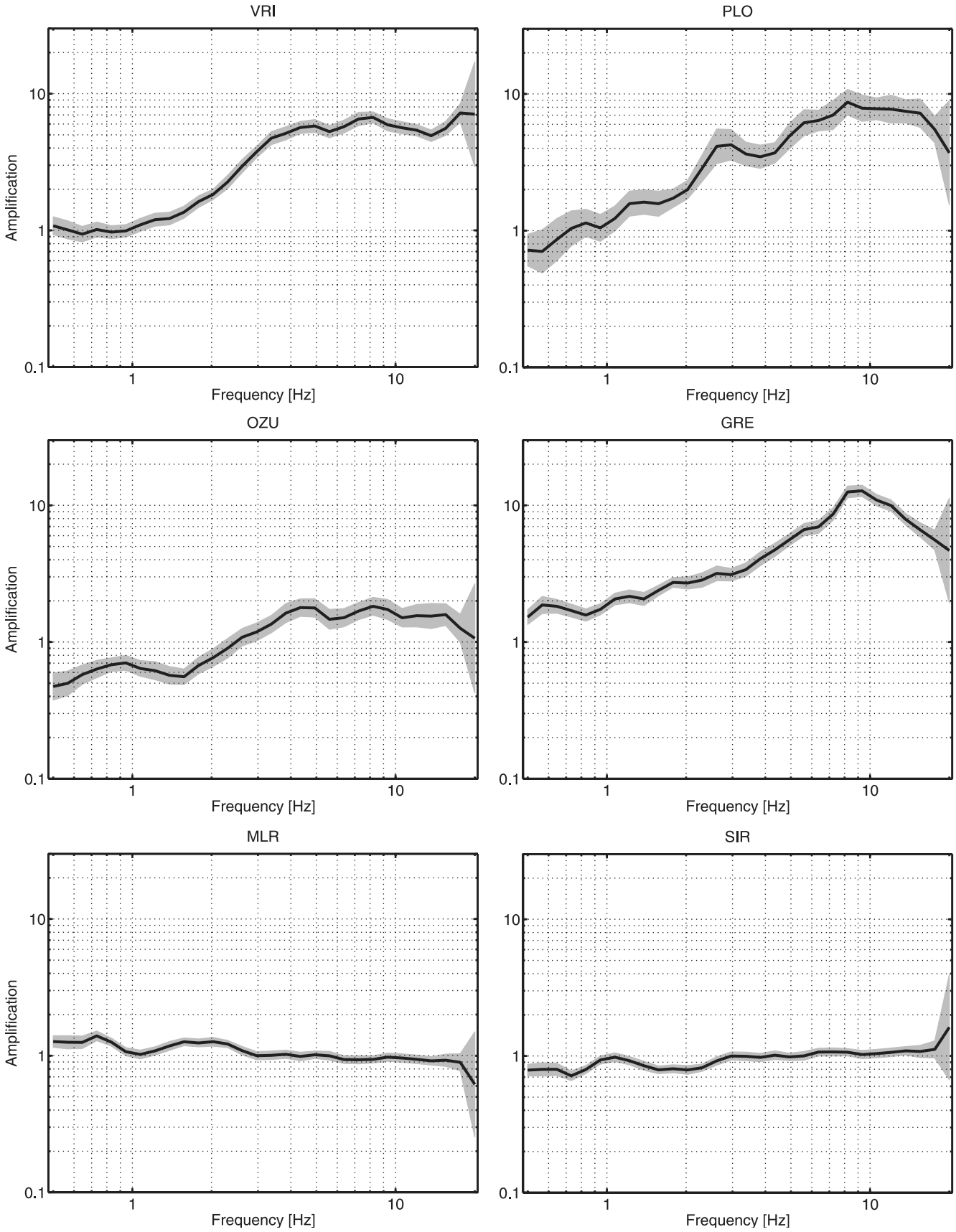

Figure 8. Site amplification functions obtained from the horizontal component at six stations in and close to the epicentral area. Black line: mean of 200 bootstrap samples. Gray shaded area: mean ± one standard deviation.

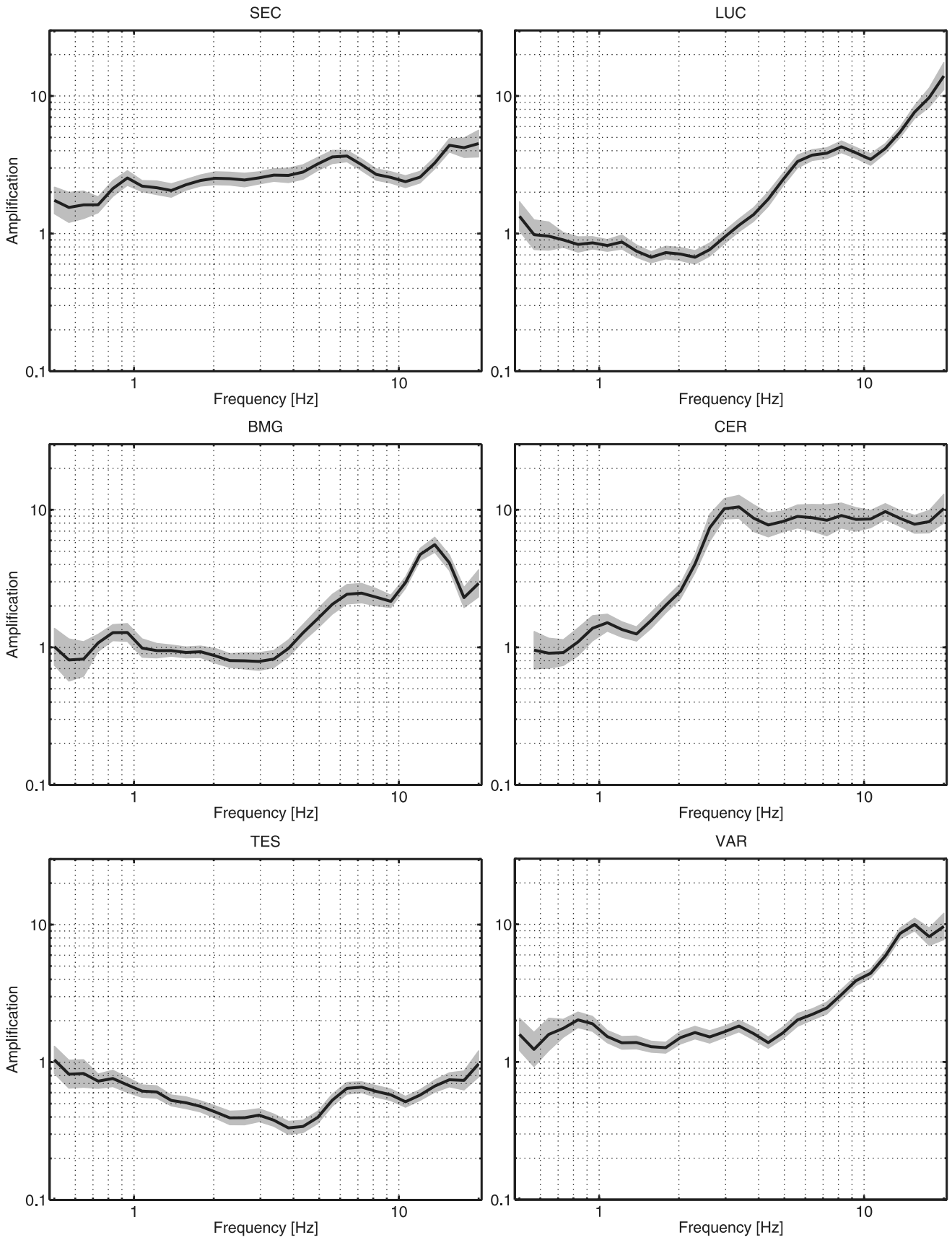

Figure 9. Site amplification functions obtained from the vertical component at six stations in the forearc region. Black line: mean of 200 bootstrap samples. Gray shaded area: mean ± one standard deviation.

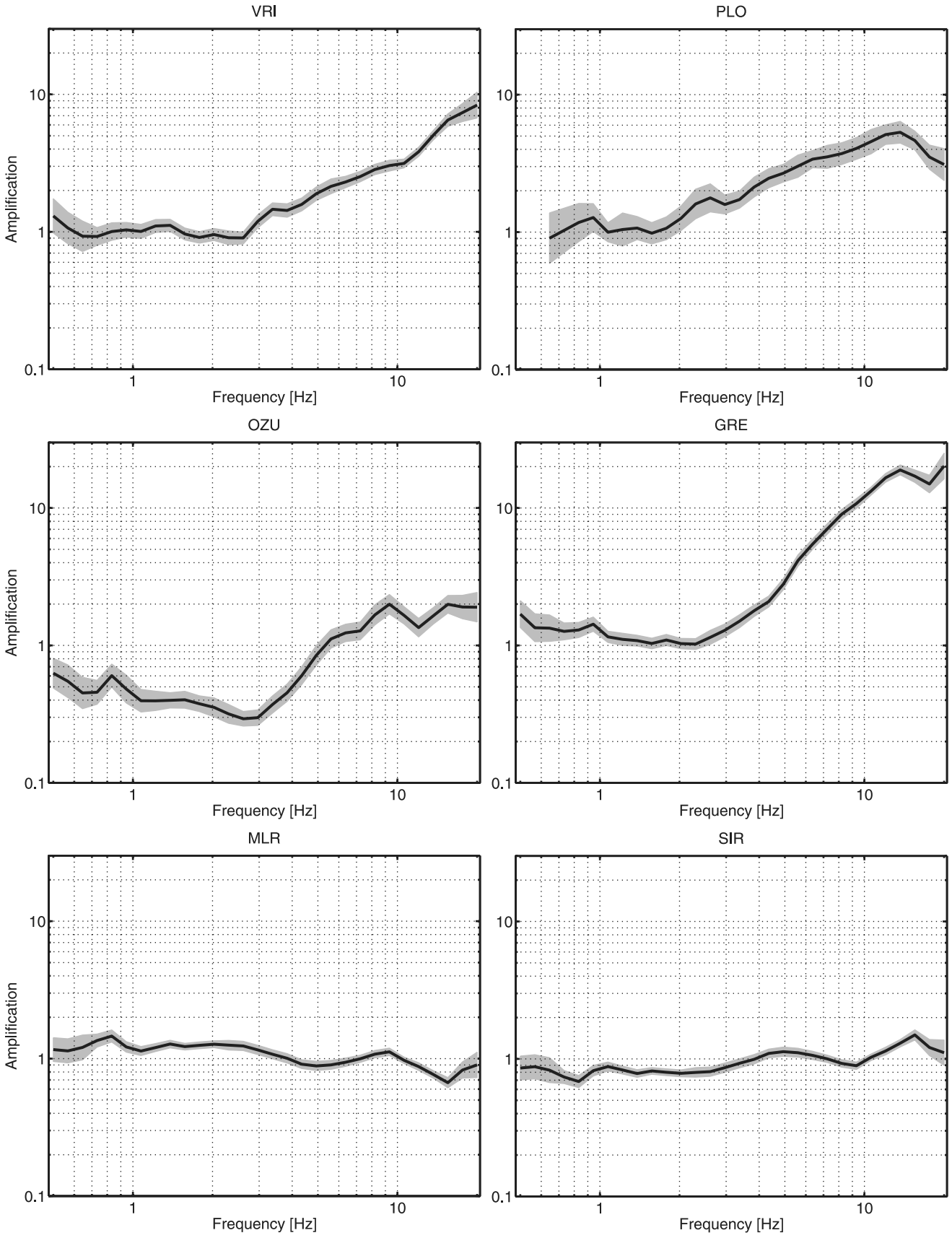

Figure 10. Site amplification functions obtained from the vertical component at six stations in and close to the epicentral area. Black line: mean of 200 bootstrap samples. Gray shaded area: mean ± one standard deviation.

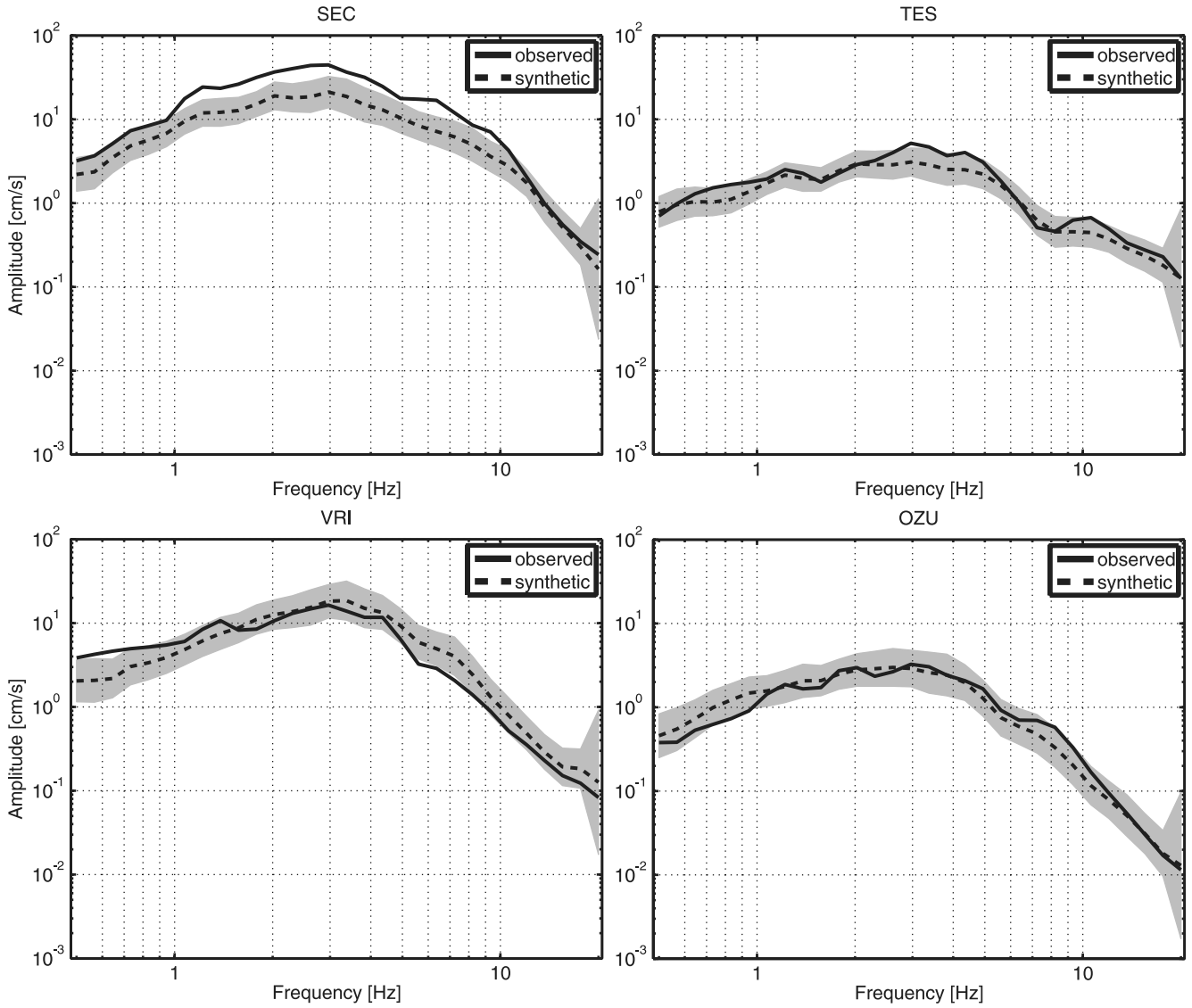

Figure 11. Example for the fit between observed (continuous line) and synthetic (dashed line) spectra generated with the inverted spectral model (attenuation functions are from Oth *et al.* [2008]; source and site spectra are from this article) for the 27 October 2004 earthquake (M_w 5.8). The gray shaded area indicates the modeled spectrum if, for source, site, and attenuation functions ±one standard deviation is taken into account.

the Z component (as the source and attenuation contributions are, in principle, included in both components). Figure 12 shows the comparison of the H/V ratios with the ratio of the site amplification functions for the H and the Z component derived by the inversion (denoted as GIT H/Z in the following) at several stations. Interestingly, the general shape of the H/V ratios can be quite well explained with the GIT H/Z ratio. For instance, the prominent peak in the H/V ratio at station CER or the peak at station LUC between 2 and 3 Hz are astonishingly similar. There is, however, a slight trend for amplitude differences at low frequencies.

Most of this difference between the GIT H/Z and the H/V ratios at low frequencies can be explained by the fact that the H/V ratios at stations MLR and SIR are not entirely flat at low frequencies but show an amplification of a factor of 1.5–3. The site constraint used in the GIT inversion, however, produces a GIT H/Z ratio approximately equal to one for these two stations. Therefore, the GIT H/Z ratios underestimate the H/V ratios at low frequencies. In Figure 13, the comparison between the H/V and the GIT H/Z ratios is shown in the case where the site constraint in the GIT inversion is set to equal the H/V ratio for MLR and to be one for MLR, when the H and Z components are considered, respectively. Therefore, for MLR, the GIT H/Z and H/V ratios are equal. For the other stations, the H/V and GIT H/Z ratios are very close to each other and depict nearly identical shapes. If the H/V ratio at MLR is used as a site constraint for the H component, all of the site functions of the H component show higher amplifications at low frequencies.

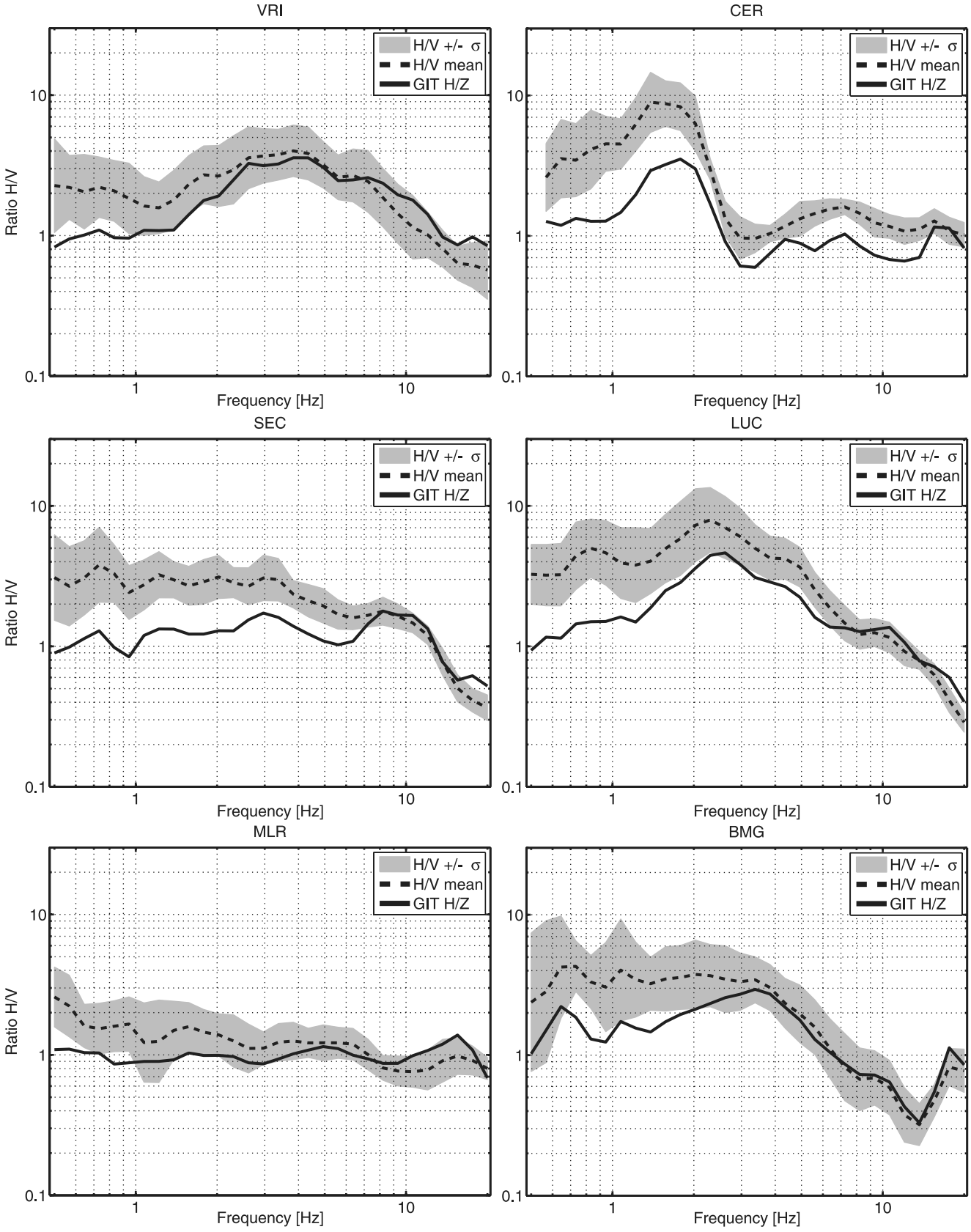

Figure 12. Comparison between H/V spectral ratios and the ratio of amplification functions H/Z obtained from the GIT at six stations. The peaks observed in the H/V spectral ratio and its general shape can be well reproduced by the GIT H/Z results. The differences, especially at low frequencies, are mostly due to the site constraint (logarithmic average of MLR and SIR equal to zero), as shown in Figure 13.

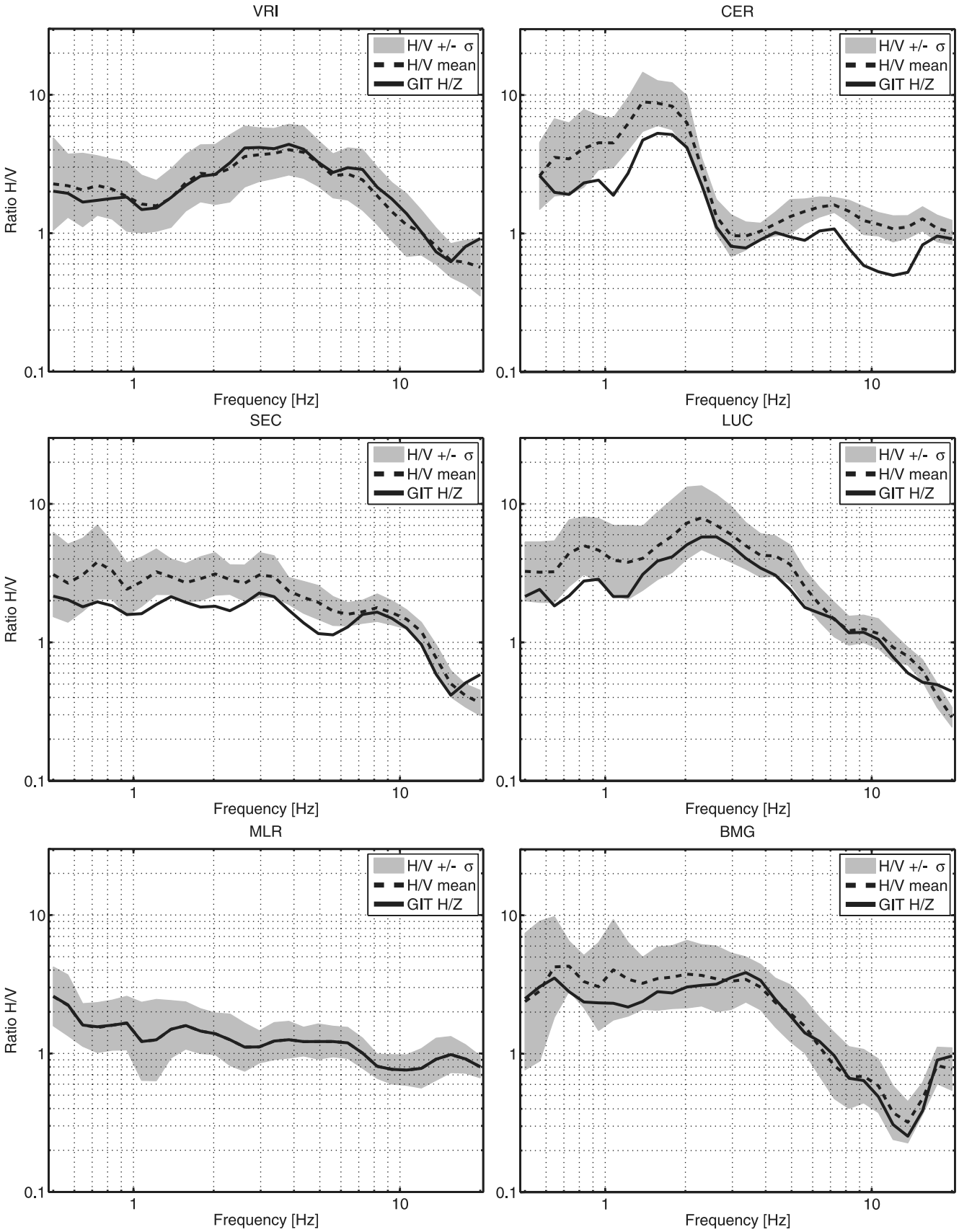

Figure 13. Comparison between H/V spectral ratios and the ratio of amplification functions H/Z obtained from GIT at six stations using the H/V ratio of MLR as a site constraint for the H component (and the Z site function constrained to one) in the GIT.

The remaining difference between GIT H/Z and H/V ratios is related to the fact that the Z component does not carry much S-wave information, in contrast to the H component. Oth *et al.* (2008) discuss seismic attenuation based on the first-step inversion of the two-step GIT approach using the H component. Yet if the first-step inversion (with the modification in the inversion scheme discussed in Oth *et al.* [2008]) is applied to the Z component spectra, different attenuation characteristics are obtained than those from the H component, especially in the forearc region. In contrast to these results, by taking the H/V ratio as an estimate of the ratio of site amplification functions for H and Z component, one assumes that both components are subjected to identical attenuation. If, additionally to the usage of the H/V ratio at station MLR as a site constraint the Z component is corrected with the same attenuation function as the H one (and not with its specific one), then the H/V and GIT H/Z ratios are exactly matching each other (not shown here). The largest part of the difference, however, is clearly attributable to the site constraint, as Figures 12 and 13 demonstrate.

These results indicate that the H/V ratio from earthquake data is not a good estimate of site amplification on the horizontal component of ground motion in the case of Vrancea earthquakes, at least not for frequencies higher than 1–2 Hz.

Discussion

Using the nonparametric GIT, we calculated source spectra and site transfer functions from the largest accelerometric dataset available for intermediate-depth Vrancea earthquakes, after correcting the FAS with the attenuation functions derived by Oth *et al.* (2008) from the same dataset.

The source spectra show high corner frequencies, which are equivalent to high stress drops of 100–200 MPa when using the Brune (1970, 1971) model. These high stress-drop values are in good agreement with the source parameter study performed by Oth *et al.* (2007) using EGF modeling and the results of Oncescu (1989) for the asperity stress release of the large Vrancea earthquake that occurred on 30 August 1986 (M_w 7.1). Furthermore, our results indicate roughly self-similar scaling among Vrancea earthquakes (Fig. 5), corroborating the findings of the spectral scaling analysis between several Vrancea events performed by Oth *et al.* (2007). However, Sokolov *et al.* (2004, 2005) come to a different conclusion and use stress-drop values increasing with magnitude. This would mean that Vrancea earthquakes would not show self-similar scaling, a result in contradiction with our findings, and we will discuss the reasons for this discrepancy later.

The site response functions obtained from the GIT depict a high level of amplification at high frequencies, and this effect is also very prominent in the Z component in many cases. Commonly, such a strong amplification at high frequencies is caused by a thin low-velocity layer over a high-speed substrate with a large impedance contrast. However, due to the lack of geotechnical information for the sites showing such a prominent amplification at high frequencies (e.g., CER or VAR), we can neither confirm nor reject this explanation. The maximum amplification is generally shifted to higher frequencies in the Z component as compared with the H component. The comparison between the GIT outcome and the H/V ratios, as previously discussed in the respective section, indicates that the H/V ratio is not a good estimate of site amplification on the H component.

Several previous studies dealt with source spectra, site effects, and seismic attenuation beneath Vrancea. Oncescu, Bonjer, *et al.* (1999) used a somewhat similar approach as presented here to separate source and site contributions from a much smaller dataset of strong (the four large Vrancea events in 1977, 1986, and 1990) and weak motion (recorded from 1985–1990) spectra from Vrancea earthquakes. They determined a $Q(f)$ model for S waves using the coda waves from two Vrancea earthquakes at station Incerc in Bucharest (finding $Q(f) = 109f^{0.81}$) and corrected the spectra for attenuation and geometrical spreading before performing the inversion for source spectra and site amplification functions. As a site constraint, they used the transfer function calculated from geotechnical data at station Incerc.

The different correction of attenuation, different site constraint, and only three common station locations between their study and ours make a direct comparison of the results difficult. However, they observe, for instance, a very strong deamplification at station MLR at high frequencies (also deamplification at VRI), which hints to differences between the attenuation model derived from coda waves and a very small amount of data in Bucharest (forearc region) and our model (Oth *et al.*, 2008) based on the S-wave part of the recordings. Indeed, Oth *et al.* (2008) show that in and close to the epicentral area, attenuation is higher by up to one order of magnitude as compared with the foreland region. With respect to sites in the foreland, the $Q(f)$ model derived by Oncescu, Bonjer, *et al.* (1999) is similar to the $Q(f)$ model derived by Oth *et al.* (2008) from the slopes of the nonparametric attenuation functions computed in the first step of the two-step GIT inversion scheme (Castro *et al.*, 1990) and hence better suited than for those stations located in the epicentral region. The fact that Oncescu, Bonjer, *et al.* (1999) used a single attenuation model for the whole area can then explain the differences with our results.

Extensive studies on the spectral properties of ground motion from Vrancea earthquakes have also been performed by Sokolov *et al.* (2004, 2005). Their approach is, however, somewhat different and does not involve an inversion procedure. Sokolov *et al.* (2005) use the H/V ratio from earthquake data as an estimate of site amplification of the horizontal component at eight rock stations that are also included in the dataset used in the aforementioned GIT. After the removal of this site effect estimate, they correct for attenuation along the path using a three-layered $Q(f)$ model that leads to slightly less attenuation than the model derived for the forearc area by Oth *et al.* (2008). However, following

the recent results of Oth *et al.* (2008), this model seems to be inappropriate for stations SIR, VRI, and OZU (which are included in their dataset and are located, following Oth *et al.* [2008], in the region of much stronger attenuation). Furthermore, Sokolov *et al.* (2004, 2005) had to introduce an additional model parameter, κ (Anderson and Hough, 1984), to account for the remaining high-frequency decay with respect to an ω^{-2} source model. The κ parameter, as it will be shown in the following, is the key to understanding the main difference between the Sokolov *et al.* (2004, 2005) model and the results presented in this study.

Compared to the results from the GIT in this article, Sokolov *et al.* (2004, 2005) underestimate the site effect at high frequencies by using the H/V ratio (as the Z component is also amplified), but also strongly underestimate attenuation along the path for high frequencies for stations located in and close to the epicentral area (region 2 in Oth *et al.* [2008]). Without the further model parameter κ accounting for this fact (in the spectral model, the term is $e^{-\pi\kappa f}$), the final high-frequency content in this area would be overestimated, because the effect of differences in attenuation and H/V would not compensate each other. Therefore, Sokolov *et al.* (2005) need to introduce rather high κ values within the mountain arc to fit the observations ($\kappa = 0.07$ for SIR, $\kappa =$ 0.04–0.07 for VRI, and $\kappa = 0.05$–0.07 for OZU). Note that κ as used by Sokolov *et al.* (2005) is not directly related to the high-frequency fall off of the observed spectra. In their study, κ explains the remaining deviation of the spectra from an ω^{-2} source spectrum after correcting for site effects using the H/V ratios and attenuation correction derived by their $Q(f)$ model. In the forearc area, their $Q(f)$ model is better suited than for sites in the epicentral area. Sokolov *et al.* (2004, 2005) use κ values as well as stress drop increasing with magnitude (as mentioned earlier) in their spectral model. In fact, these are two counteracting effects, as the increase of the high-frequency spectral level due to the increase of the stress drop (and hence, corner frequency) is reduced again by increasing the value of κ.

In our study, as mentioned earlier, no κ operator has been included into the site constraint for the rock stations. Introducing such an operator into the site constraint in the GIT inversion would lead to less severe amplification at high frequencies for all site response functions, but relative to each other, the site amplification functions would show the same characteristic features, that is, strong amplification at high frequencies relative to the reference sites. However, differences in κ between different sites should be included in the derived site response functions. The missing κ term for the rock stations, which would lead to the same additional decay of all the site responses at high frequencies, is moved into the source contributions, an issue that has been discussed in detail in the Source Spectra of Vrancea Earthquakes section.

Yet both models, the one of Sokolov *et al.* (2004, 2005) as well as the GIT results presented in Oth *et al.* (2008) and in this article, are able to explain the observed spectra and are suitable for practical application. The key question is the physical interpretation of the results. Here, the implications of the models are radically different. Because Oth *et al.* (2008) showed the necessity of using different attenuation relationships for different source-to-receiver paths (a similar correction is only done *a posteriori* by Sokolov *et al.* (2004, 2005) introducing the κ parameter with strongly varying values between different clusters of stations, i.e., within the mountain arc and in the foreland) that are in agreement with the knowledge about the deep structure of the Vrancea region, our results indicate that, using an inversion procedure, the contributions of source, path, and site to the final ground motion can be better isolated avoiding too restrictive constraints (e.g., that the H/V ratio is representative of the site response) and *a posteriori* adjustment to the model. This yields results providing different insights on the physical processes generating the observed ground motion. It is, for instance, remarkable that differently from Sokolov *et al.* (2004, 2005), no increase of stress drop with magnitude was observed, hinting to self-similar scaling.

The attenuation characteristics were not assumed to be given by a certain $Q(f)$ model, but empirically derived in a first step (Oth *et al.*, 2008) from the dataset. Thus, the attenuation correction performed before the second step inversion is certainly in agreement with this specific dataset. For the second step, the only assumption made is the amplification at the rock sites MLR and SIR. As mentioned earlier, the H/V ratios are roughly flat for these sites with level unity, which means that at least both the H and Z component are amplified in the same way. However, considering the fact that these are rock sites, assuming unit site response seems to be well justified. The strongest assumption made in this study is the usage of a reference source spectrum for the 27 October 2004 (M_w 5.8) earthquake to correct for the effect of the reference distance in the inverted source contributions. However, as this event is the Vrancea earthquake with the largest amount of high-quality recordings and its source characteristics have been studied in detail (Oth *et al.*, 2007), this is clearly the best choice as a reference event. Moreover, this assumption is not directly linked to the inversion procedure, but only to the interpretation of the inverted source contributions.

Conclusions

We investigated the source spectra and site amplification functions from a dataset of 55 intermediate-depth Vrancea earthquakes recorded at 43 stations spread over Romanian territory. Because of the clustering of the hypocenters in a very small focal volume at intermediate depth, the lowest hypocentral distance in the dataset ranges around 90 km and there are only few crossing ray paths from the source region to the different stations.

The main implication of the few ray crossings is that lateral variations in seismic attenuation are not averaged out, as discussed by Oth *et al.* (2008), and must be taken into

account when developing spectral ground-motion models for the region. In this article, we separated the attenuation-corrected spectra into their source and site contributions. As we used a site constraint in the inversion, the inverted source spectra are still subjected to seismic attenuation over the reference distance of 90 km. This effect can be corrected when the source spectrum of a reference earthquake is known, and we used the 27 October 2004 (M_w 5.8) Vrancea earthquake as a reference event. The final source spectra depict large corner frequencies and, consequently, large Brune (1970, 1971) stress drops of the order of 100 MPa, which is an order of magnitude larger than expected from typical crustal earthquakes of the same size. Furthermore, Vrancea earthquakes seem to show a roughly self-similar scaling behavior. These high corner frequencies indicate a very efficient high-frequency radiation and corroborate the results on the source characteristics of several Vrancea earthquakes obtained by Oth *et al.* (2007) with an EGFs study.

The site amplification functions obtained from the inversion depict strong amplification effects at high frequencies at most stations, both on the horizontal and vertical components. A comparison of the H/V ratios computed from the shear-wave windows and the site amplification functions obtained by GIT inversion clearly reveal that the H/V ratios are not a good estimate of site amplification on the horizontal component. By computing the ratio of the horizontal to vertical site amplification functions estimated from the GIT, the H/V ratios can be well reproduced. Because of the large amplification on the vertical component at most stations, the H/V ratios systematically underestimate the amplification at high frequencies.

Finally, the spectral ground-motion models composed of the attenuation functions derived by Oth *et al.* (2008) and the source spectra and site amplification functions presented in this article can be used as a basis for stochastic simulations of ground motions resulting from scenario earthquakes and are thus a valuable contribution in view of seismic hazard assessment for Romania.

Data and Resources

The seismograms used in this study were collected by instruments of the strong-motion network deployed in Romania since 1997 in the framework of the CRC 461 "Strong Earthquakes: A Challenge for Geosciences and Civil Engineering" of the University of Karlsruhe in collaboration with the NIEP in Bucharest. The recordings from the three large Vrancea events that occurred in 1986 and 1990 were obtained from an analog SMA-1 network and digitized at NIEP. The data may be obtained from the authors upon request. The hypocentral coordinates of the analyzed events have been taken from the ROMPLUS catalog (Oncescu, Marza, *et al.*, 1999), which is continuously updated as new earthquakes occur and is available at http://www.infp.ro/catal.php.

Acknowledgments

This study was carried out in the CRC 461 "Strong Earthquakes: A Challenge for Geosciences and Civil Engineering," which is funded by the Deutsche Forschungsgemeinschaft (German Research Foundation) and supported by the state of Baden–Württemberg and the University of Karlsruhe. The authors wish to thank Art McGarr, Raúl R. Castro, and an anonymous referee for beneficial comments and suggestions that helped to improve the article.

References

Anderson, J. G., and E. S. Hough (1984). A model for the shape of the Fourier amplitude spectrum of acceleration at high frequencies, *Bull. Seismol. Soc. Am.* **74,** 1969–1993.

Andrews, D. J. (1986). Objective determination of source parameters and similarity of earthquakes of different size, in *Earthquake Source Mechanics*, S. Das, J. Boatwright and C. H. Scholz (Editors), American Geophysical Monograph **37,** 259–267.

Beresnev, I. A. (2001). What we can and cannot learn about earthquake sources from the spectra of seismic waves, *Bull. Seismol. Soc. Am.* **91,** 397–400.

Beresnev, I. A. (2002). Source parameters observable from the corner frequency of earthquake spectra, *Bull. Seismol. Soc. Am.* **92,** 2047–2048.

Bindi, D., S. Parolai, H. Grosser, C. Milkereit, and S. Karakisa (2006). Crustal attenuation characteristics in northwestern Turkey in the range from 1 to 10 Hz, *Bull Seismol. Soc. Am.* **96,** 200–214.

Bonilla, L. F., J. H. Steidl, G. T. Lindley, A. G. Tumarkin, and R. J. Archuleta (1997). Site amplification in the San Fernando Valley, California: variability of site-effect estimation using the *S*-wave, coda and H/V methods, *Bull. Seismol. Soc. Am.* **87,** 710–730.

Boore, D. M. (2003). Simulation of ground motion using the stochastic method, *Pure Appl. Geophys.* **160,** 635–676.

Boore, D. M., and W. B. Joyner (1997). Site amplifications for generic rock studies, *Bull. Seismol. Soc. Am.* **87,** 327–341.

Brune, J. N. (1970). Tectonic stress and the spectra of seismic shear waves from earthquakes, *J. Geophys. Res.* **75,** 4997–5009.

Brune, J. N. (1971). Correction, *J. Geophys. Res.* **76,** 5002.

Castro, R. R., J. G. Anderson, and S. K. Singh (1990). Site response, attenuation and source spectra of *S* waves along the Guerrero, Mexico, subduction zone, *Bull. Seismol. Soc. Am.* **80,** 1481–1503.

Chen, S.-Z., and G. M. Atkinson (2002). Global comparisons of earthquake source spectra, *Bull. Seismol. Soc. Am.* **92,** 885–895.

Cioflan, C. O., B. F. Apostol, C. L. Moldoveanu, G. F. Panza, and G. Marmureanu (2004). Deterministic approach for the seismic microzonation of Bucharest, in *Seismic Ground Motion in Large Urban Areas*, Pageoph Topical Volumes, Vol. **161**, G. F. Panza, I. Paskaleva and C. Nunziata (Editors), Birkhäuser, Basel.

Constantinescu, L., and D. Enescu (1964). Fault-plane solutions for some Romanian earthquakes and their seismotectonic implication, *J. Geophys. Res.* **69,** 667–674.

Efron, B., and R. J. Tibshirani (1994). *An Introduction to the Bootstrap*, Chapman and Hall, London.

Field, E. H., and K. H. Jacob (1995). A comparison and test of various site response estimation techniques including three that are not reference-site dependent, *Bull. Seismol. Soc. Am.* **85,** 1127–1143.

García, D., S. K. Singh, M. Herráiz, J. F. Pacheco, and M. Ordaz (2004). Inslab earthquakes of Central Mexico: Q, source spectra and stress drop, *Bull. Seismol. Soc. Am.* **94,** 789–802.

Hanks, T. C. (1982). f_{max}, *Bull. Seismol. Soc. Am.* **72,** 1867–1879.

Hanks, T. C., and H. Kanamori (1979). A moment magnitude scale, *J. Geophys. Res.* **84,** 2348–2350.

Hartzell, S. H., A. Leeds, A. Frankel, and J. Michael (1996). Site response for urban Los Angeles using aftershocks of the Northridge earthquake, *Bull. Seismol. Soc. Am.* **86,** S168–S192.

Hauser, F., V. Raileanu, W. Fielitz, C. Dinu, M. Landes, A. Bala, and C. Prodehl (2007). Seismic crustal structure between the Transylvanian basin and the Black Sea, Romania, *Tectonophysics* **430,** 1–25.

Kanamori, H. (1994). Mechanics of earthquakes, *Ann. Rev. Earth Planet. Sci.* **22,** 207–237.

Konno, K., and T. Ohmachi (1998). Ground-motion characteristics estimated from spectral ratio between horizontal and vertical components of microtremor, *Bull. Seismol. Soc. Am.* **88,** 228–241.

Lermo, J., and F. J. Chávez-García (1993). Site effect evaluation using spectral ratios with only one station, *Bull. Seismol. Soc. Am.* **83,** 1574–1594.

Martin, M., F. Wenzel, and the CALIXTO Working Group (2006). High resolution teleseismic body wave tomography beneath SE-Romania (II): imaging of a slab detachment scenario, *Geophys. J. Int.* **164,** 579–595.

Menke, W. (1989). *Geophysical Data Analysis: Discrete Inverse Theory*, International Geophysics Series, Academic Press, New York.

Miyake, H., T. Iwata, and K. Irikura (2003). Source characterization for broadband ground-motion simulations: kinematic heterogeneous source model and strong motion generation area, *Bull. Seismol. Soc. Am.* **93,** 2531–2545.

Nakamura, Y. (1989). A method for dynamic characteristics estimation of subsurface using microtremor on the ground surface, *QR Railw. Tech. Res. Inst.* **30,** 25–33.

Oncescu, M. C. (1989). Investigation of a high stress drop earthquake on August 30, 1986 in the Vrancea region, *Tectonophysics* **163,** 35–43.

Oncescu, M. C., and K.-P. Bonjer (1997). A note on the depth recurrence and strain release of large Vrancea earthquakes, *Tectonophysics* **272,** 291–302.

Oncescu, M. C., K.-P. Bonjer, and M. Rizescu (1999). Weak and strong ground motion of intermediate depth earthquakes from the Vrancea region, in *Vrancea Earthquakes: Tectonics, Hazard and Risk Mitigation*, F. Wenzel, D. Lungu and O. Novak (Editors), Kluwer Academic Publishers, Dordrecht, 27–42.

Oncescu, M. C., V. I. Marza, M. Rizescu, and M. Popa (1999). The Romanian earthquake catalogue between 984–1997, in *Vrancea Earthquakes: Tectonics, Hazard and Risk Mitigation*, F. Wenzel, D. Lungu and O. Novak (Editors), Kluwer Academic Publishers, Dordrecht, 43–48.

Oth, A., F. Wenzel, and M. Radulian (2007). Source parameters of intermediate-depth Vrancea (Romania) earthquakes from empirical Green's functions modeling, *Tectonophysics* **438,** 33–56.

Oth, A., D. Bindi, S. Parolai, and F. Wenzel (2008). *S*-wave attenuation characteristics beneath the Vrancea region in Romania: new insights from the inversion of ground-motion spectra, *Bull. Seismol. Soc. Am.* **98,** no. 5, 2482–2497, doi: 10.1785/0120080106.

Papageorgiou, A. S., and K. Aki (1983). A specific barrier model for the quantitative description of inhomogeneous faulting and prediction of strong motion, part I: description of the model, *Bull. Seismol. Soc. Am.* **73,** 693–722.

Parolai, S., and D. Bindi (2004). Influence of soil-layer properties on k evaluation, *Bull. Seismol. Soc. Am.* **94,** 349–356.

Parolai, S., and S. M. Richwalski (2004). The importance of converted waves in comparing H/V and RSM site response estimates, *Bull. Seismol. Soc. Am.* **94,** 304–313.

Parolai, S., D. Bindi, and P. Augliera (2000). Application of the generalized inversion technique (GIT) to a microzonation study: numerical simulations and comparison with different site-estimation techniques, *Bull. Seismol. Soc. Am.* **90,** 286–297.

Parolai, S., D. Bindi, M. Baumbach, H. Grosser, C. Milkereit, S. Karakisa, and S. Zünbül (2004). Comparison of different site response estimation techniques using aftershocks of the 1999 Izmit earthquake, *Bull. Seismol. Soc. Am.* **94,** 1096–1108.

Purvance, M. D., and J. G. Anderson (2003). A comprehensive study of the observed spectral decay in strong-motion accelerations recorded in Guerrero, Mexico, *Bull. Seismol. Soc. Am.* **93,** 600–611.

Siddiqqi, J., and G. M. Atkinson (2002). Ground-motion amplification at rock sites across Canada as determined from the horizontal-to-vertical component ratio, *Bull. Seismol. Soc. Am.* **90,** 877–884.

Sokolov, V., K.-P. Bonjer, and F. Wenzel (2004). Accounting for site effect in probabilistic assessment of seismic hazard for Romania and Bucharest: a case of deep seismicity in Vrancea zone, *Soil Dyn. Earthquake Eng.* **24,** 929–947.

Sokolov, V., K.-P. Bonjer, M. Onescu, and M. Rizescu (2005). Hard rock spectral models for intermediate depth Vrancea (Romania) earthquakes, *Bull. Seismol. Soc. Am.* **95,** 1749–1765.

Sperner, B., F. P. Lorenz, K.-P. Bonjer, S. Hettel, B. Müller, and F. Wenzel (2001). Slab break-off—abrupt cut or gradual detachment? new insights from the Vrancea region (SE Carpathians, Romania), *Terra Nova* **13,** 172–179.

Theodulidis, N., and P.-Y. Bard (1995). Horizontal to vertical spectral ratio and geological conditions: an analysis of strong motion data from Greece and Taiwan, *Soil. Dyn. Earthquake Eng.* **14,** 177–197.

European Center for Geodynamics and Seismology
Rue Josy Welter, 19
L-7256 Walferdange
Grand-Duchy of Luxembourg
adrien.oth@ecgs.lu
(A.O.)

Helmholtz Centre Potsdam
GFZ German Research Centre for Geosciences
Telegrafenberg
14473 Potsdam, Germany
(S.P.)

Istituto Nazionale di Geofisica e Vulcanologia
Via Bassini, 15
20133 Milano, Italy
(D.B.)

Geophysical Institute
University of Karlsruhe
Hertzstrasse 16
76187 Karlsruhe, Germany
(F.W.)

Manuscript received 7 May 2008